Unique three-phase states in $(1-x)$Pb(Zn$_{1/3}$Nb$_{2/3}$)O$_3$–xPbTiO$_3$ single crystals

Unique three-phase states in $(1-x)\text{Pb}(\text{Zn}_{1/3}\text{Nb}_{2/3})\text{O}_3–x\text{PbTiO}_3$ single crystals

V Yu Topolov[1]

Forschungszentrum Karlsruhe GmbH in der Helmholtz-Gemeinschaft, Institut für Materialforschung II, Postfach 36 40, D-76021 Karlsruhe, Germany

E-mail: topolov@phys.rsu.ru

Abstract
This paper reports results on the crystallographic study of heterophase structures in relaxor–ferroelectric $(1-x)\text{Pb}(\text{Zn}_{1/3}\text{Nb}_{2/3})\text{O}_3–x\text{PbTiO}_3$ single crystals with $0.06 < x < 0.11$. Possible variants of the elastic matching of three ferroelectric polydomain or twinned phases are considered with due regard for the relief of internal stresses at various volume fractions of these phases near the morphotropic phase boundary. It is found that two-phase regions, 'rhombohedral–monoclinic' and 'monoclinic–tetragonal', can be elastically matched along so-called zero-net-strain planes, parallel to the (100) or (010) domain (twin) walls in the intermediate monoclinic phase, where the Miller indices (hkl) are written in terms of the perovskite axes of the cubic unit cell. Calculated volume fractions of the three phases coexisting at $0.06 < x < 0.11$ agree well with recent experimental results obtained by Bertram *et al* (2003 *J. Cryst. Growth* **253** 212).

1. Introduction

The relaxor-based $(1-x)\text{Pb}(\text{Zn}_{1/3}\text{Nb}_{2/3})\text{O}_3–x\text{PbTiO}_3$ (PZN–PT) solid solutions with the perovskite-type structure have been intensively studied in the last few years due to the very high piezoelectric activity [1–5], the various domain (or twinned) and heterophase structures [6–11] and the presence of intermediate monoclinic or orthorhombic phases [2, 12–17]. These and related phenomena are observed in PZN–PT single crystals near the morphotropic phase boundary, i.e., in the range of molar concentrations $x \approx 0.08$–0.10. Our previous attempts to investigate the heterophase structures in these single crystals were restricted to cases of the coexistence of two ferroelectric phases, such as rhombohedral (Rh) $R3m$–tetragonal

[1] Permanent address: Department of Physics, Rostov State University, 5 Zorge Street, 344090 Rostov-on-Don, Russia.
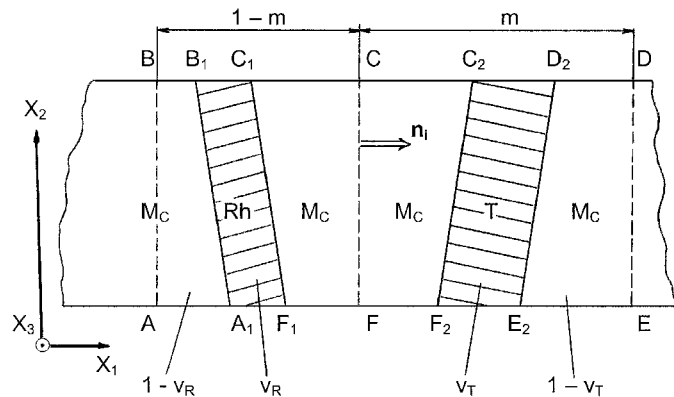
Figure 1. A cross-section of a three-phase single crystal through the (X_1OX_2) plane. n_i: normal vector of the interface CF between the two-phase ABCF and CDEF regions.

(T) $P4mm$ [4, 7, 10], Rh–monoclinic (M_C in the notation of [2]) [10], M_C–T [19] and orthorhombic–T [11]. In our works [4, 7, 10, 11], different variants of non-180° domain structures in the above-mentioned ferroelectric phases were examined as regards whether they satisfy the conditions for zero-net-strain planes (ZNSPs) [18, 19] at the elastic matching of the two phases.

In the meantime, recent experimental results [17] have shown that the M_C phase with Pm symmetry coexists with both the Rh and T phases over a wide range of x values at room temperature and the dependence of the volume fraction of the M_C phase on x is non-monotonic, in contrast to the dependences found for the Rh and T phases. Earlier we analysed features of the three-phase states 'T $P4mm$–Rh $R3m$–cubic $Pm3m$' in ferroelectric $Pb(Zr_{1-x}Ti_x)O_3$ single crystals by using the crystallographic [20] and thermodynamic [21] methods. After these studies, as the intermediate monoclinic (M_A in the notation of the review [2]) Cm phase was experimentally revealed and investigated in $Pb(Zr_{1-x}Ti_x)O_3$ [22], the role of the M_A phase in the elastic matching and the stress relief was also analysed [23]. In the work [23], different variants of the ZNSPs and corresponding optimal domain volume fractions were determined only for the two-phase states (i.e., T–Rh, Rh–M_A and T–M_A) close to the morphotropic phase boundary of the $Pb(Zr_{1-x}Ti_x)O_3$ solid solutions. In this connection, the present paper is aimed at the development of model concepts for the three-phase states in ferroelectric materials and the determination of optimal volume fractions of the phases coexisting in the PZN–PT single crystals near the morphotropic phase boundary.

2. Elastic matching of heterophase regions

In order to analyse the three-phase states and related elastic effects in the PZN–PT system, we propose the following model. The stress-free single crystal is represented as a set of two types of heterophase region, ABCF and CDEF (figure 1). Each region consists of a matrix (the intermediate M_C phase) and a plate-like inclusion (the Rh or T phase that is situated to the left or right of the morphotropic phase boundary [17], respectively). The volume fraction of the Rh inclusion ($A_1B_1C_1F_1$) in the ABCF region is v_R whereas the T inclusion ($C_2D_2E_2F_2$) in the CDEF region is characterized by the volume fraction v_T. We assume that the above-mentioned regions are uniformly distributed in the crystal sample and their volume fractions equal m

(CDEF) and $1-m$ (ABCF). The phases coexisting in the crystal sample are described by the volume fractions m_R (Rh phase), m_M (M_C phase) and m_T (T phase) as follows:

$$m_R = (1-m)v_R \qquad m_M = (1-m)(1-v_R) + m(1-v_T) \qquad m_T = m v_T. \tag{1}$$

For the description of domain types in each phase, a rectangular coordinate system (X_1, X_2, X_3) is introduced (figure 1); the axes of this system are assumed to be parallel to the perovskite unit-cell vectors in the paraelectric cubic ($Pm3m$) phase of PZN–PT. Orientations of individual ferroelectric domains as components of mechanical twins in the Rh, M_C and T phases are given by unit-cell vectors ($\mathbf{a}$, $\mathbf{b}$, $\mathbf{c}$) in the (X_1, X_2, X_3) system. These domains are separated by stress-free planar walls (or domain boundaries) whose orientations are determined according to results of works by Fousek and Janovec [24].

In the Rh phase, four types of 71° (109°) domain are characterized by the unit-cell vectors ($\mathbf{a_{Rd}}$, $\mathbf{b_{Rd}}$, $\mathbf{c_{Rd}}$) and volume fractions h_{Rd}, where $d = 1, 2, 3$ and 4. The above-mentioned vectors are arranged by taking into account the unit-cell shear angles [16, 17] approximately along the following directions [8, 25] in the perovskite unit cell: ([100]; [010]; [001]) ($d = 1$), ([$\bar{1}$00]; [010]; [00$\bar{1}$]) ($d = 2$), ([0$\bar{1}$0]; [$\bar{1}$00]; [00$\bar{1}$]) ($d = 3$) and ([010]; [$\bar{1}$00]; [001]) ($d = 4$). The volume concentrations of these domain types are described by two parameters [10, 19], $0 \leqslant u_R \leqslant 1$ and $0 \leqslant g_R \leqslant 1$, as follows: $h_{R1} = (1-u_R)(1-g_R)$, $h_{R2} = (1-u_R)g_R$, $h_{R3} = u_R(1-g_R)$ and $h_{R4} = u_R g_R$. In the T phase, there are two types of 90° domain with the unit-cell vectors ($\mathbf{a_{Tj}}$, $\mathbf{b_{Tj}}$, $\mathbf{c_{Tj}}$) lying along the directions ([100]; [010]; [001]) ($j = 1$, volume concentration $0 \leqslant h_T \leqslant 1$) and ([010]; [001]; [100]) ($j = 2$, volume concentration $1-h_T$). The M_C phase is characterized by four domain types [10, 12] with the unit-cell vectors ($\mathbf{a_{Ms}}$, $\mathbf{b_{Ms}}$, $\mathbf{c_{Ms}}$) lying along the directions ([010]; [010]; [001]) ($s = 1$), ([$\bar{1}$00]; [0$\bar{1}$0]; [001]) ($s = 2$), ([010]; [$\bar{1}$00]; [001]) ($s = 3$) and ([0$\bar{1}$0]; [100]; [001]) ($s = 4$). Analogously to the case of the polydomain Rh phase, the volume fractions h_{Ms} of the domains in the M_C phase are expressed in terms of two parameters, $0 \leqslant f_M \leqslant 1$ and $0 \leqslant p_M \leqslant 1$, by the formulae $h_{M1} = f_M p_M$, $h_{M2} = (1-f_M)p_M$, $h_{M3} = f_M(1-p_M)$ and $h_{M4} = (1-f_M)(1-p_M)$.

In order to analyse the elastic matching of the phases and the heterophase regions (figure 1), we write the distortion matrices of the polydomain Rh, T and M_C phases in terms from the works [10, 19, 20, 23] as

$$\|N_R\| = \begin{pmatrix} \mu_a & \mu(2g_R-1) & \mu(2u_R-1)(2g_R-1) \\ \mu(2g_R-1) & \mu_a & \mu(2u_R-1) \\ \mu(2u_R-1)(2g_R-1) & \mu(2u_R-1) & \mu_a \end{pmatrix} \tag{2}$$

$$\|N_T\| = h_T \begin{pmatrix} \varepsilon_a & 0 & 0 \\ 0 & \varepsilon_a & 0 \\ 0 & 0 & \varepsilon_c \end{pmatrix} + (1-h_T) \begin{pmatrix} \cos\varphi_T & 0 & -\sin\varphi_T \\ 0 & 1 & 0 \\ \sin\varphi_T & 0 & \cos\varphi_T \end{pmatrix} \begin{pmatrix} \varepsilon_c & 0 & 0 \\ 0 & \varepsilon_a & 0 \\ 0 & 0 & \varepsilon_a \end{pmatrix} \tag{3}$$

and

$$\|N_M\| = p_M \begin{pmatrix} \eta_a & 0 & \eta(2f_M-1) \\ 0 & \eta_b & 0 \\ 0 & 0 & \eta_c \end{pmatrix}$$
$$+ (1-p_M) \begin{pmatrix} \cos\varphi_M & -\sin\varphi_M & 0 \\ \sin\varphi_M & \cos\varphi_M & 0 \\ 0 & 0 & 1 \end{pmatrix} \begin{pmatrix} \eta_b & 0 & 0 \\ 0 & \eta_a & \eta(2f_M-1) \\ 0 & 0 & \eta_c \end{pmatrix} \tag{4}$$

respectively. The unit-cell distortions μ_a, μ from equation (2), ε_a, ε_c from equation (3), as well as η_a, η_b, η_c and η from equation (4), are expressed [10, 19] in terms of the unit-cell parameters, a_R and ω_R of the Rh phase, a_T and c_T of the T phase, a_M, b_M, c_M and ω_M of the M_C phase and a_C of the cubic phase, as follows: $\mu_a = a_R\cos\omega_R/a_C$, $\mu = a_R\sin\omega_R/a_C$, $\varepsilon_a = a_T/a_C$, $\varepsilon_c = c_T/a_C$, $\eta_a = a_M\cos\omega_M/a_C$, $\eta_b = b_M/a_C$, $\eta_c = c_M/a_C$, and $\eta = a_M\sin\omega_M/a_C$. The

angles $\varphi_T = \arccos[2\varepsilon_a\varepsilon_c/(\varepsilon_a^2+\varepsilon_c^2)]$ and $\varphi_M = \arccos[2\eta_a\eta_b/(\eta_a^2+\eta_b^2)]$ in formulae (3) and (4) are introduced for taking into account a rotation of the crystallographic axes [18, 19, 23] of the adjacent domains ($j = 1, 2$) in the T phase or domain pairs ($s = 1, 2$ and 3, 4) in the M_C phase because $\varepsilon_a \neq \varepsilon_c$ and $\eta_a \neq \eta_b$, respectively. It is assumed that the Rh and M_C phases coexisting in the ABCF region as well as the adjacent T and M_C phases in the CDEF region (figure 1) are separated by interfaces which are ZNSPs in accordance with conditions formulated in the works [10, 18, 19]. In this case, we can consider the crystal sample as a set of regions like two adjacent polydomain phases that contain permissible [24] domain walls (i.e., the internal interfaces being ZNSPs). Hereafter we write the distortion matrices of the ABCF and CDEF regions as

$$\|K^{(1)}\| = v_R\|K^{(2)}\| \cdot \|N_R\| + (1 - v_R)\|N_M\| \tag{5}$$

and

$$\|K^{(2)}\| = v_T\|K^{(1)}\| \cdot \|N_T\| + (1 - v_T)\|N_M\| \tag{6}$$

respectively. The involvement of the $\|K^{(t)}\|$ matrices in the right-hand sides of equations (5) and (6) is connected with the electromechanical interaction [11] between the ferroelectric phases in each heterophase region. The similar items containing $\|N_M\|$ in equations (5) and (6) are related to the intermediate M_C phase that plays the role of the matrix and/or the adjacent phase in both the ABCF and CDEF regions (figure 1).

Our analysis of the elastic matching of the regions of the ABCF and CDEF types in the whole crystal sample is based on the crystallographic algorithm [18] and using the matrix elements

$$D_{br} = \sum_{w=1}^{3} (K_{bw}^{(2)}K_{rw}^{(2)} - K_{bw}^{(1)}K_{rw}^{(2)}) \tag{7}$$

expressed through the matrix elements $K_{bw}^{(t)}$ ($t = 1, 2$) from equations (5) and (6). These regions are separated by the interfaces which are ZNSPs under conditions

$$\det\|D_{br}\| = 0 \qquad \text{and} \qquad D_{br}'^2 = D_{br}^2 - D_{bb}D_{rr} \geqslant 0 \qquad (b \neq r). \tag{8}$$

Orientations of these interfaces are given by normal vectors $\boldsymbol{n}_1(h_1k_1l_1) \perp \boldsymbol{n}_2(h_2k_2l_2)$ in terms of the perovskite axes of the cubic unit cell, where the Miller indices are expressed [18] by the ratios

$$h_{1,2} = D_{11}/D_{1,2} \qquad k_{1,2} = (D_{12} \pm D_{12}')/D_{1,2} \qquad l_{1,2} = (D_{13} \pm D_{13}')/D_{1,2}. \tag{9}$$

In equations (9), the matrix elements (7) and (8) or their combinations, such as $D_{1,2} = [D_{11}^2+(D_{12}\pm D_{12}')^2+(D_{13}\pm D_{13}')^2]^{1/2}$, are introduced. If the matrix elements from equation (7) do not obey at least one of conditions (8), the interfaces between the ABCF and CDEF regions become strained and may be approximated as second-degree surfaces in accordance with the results of [19, 26].

3. Results of calculations and discussion

In this section we present some results on the three-phase states and the elastic matching of the heterophase regions. Among the experimental data [17] on the PZN–PT single crystals at room temperature, we have chosen the unit-cell parameters at the following molar concentrations: $x_R = 0.06$ (the Rh phase, the left side of the concentration range), $x_M = 0.08$ (the M_C phase, the middle part of the concentration range where no changes in the unit-cell parameters are observed) and $x_T = 0.11$ (the T phase, the right side of the concentration range).

To the best of our knowledge, experimental works on PZN–PT and related solid solutions do not contain data on densities of the morphotropic phases or on interconnections between the molar concentration x of the heterophase single crystal and the volume fraction m of the two-phase CDEF-type region shown in figure 1. Faced with this fact, we assume that the effective molar concentration of the three-phase PZN–PT single crystals can be evaluated in a general form as

$$x_{\text{eff}} = m_{\text{R}}x_{\text{R}} + m_{\text{M}}x_{\text{M}} + m_{\text{T}}x_{\text{T}} \tag{10}$$

where the volume fractions m_{R}, m_{M} and m_{T} are determined according to formulae (1). As for the link $m \leftrightarrow x$, we simply assume that a linear approximation for $m = m(x)$ is possible in the range $[x_{\text{R}}; x_{\text{T}}]$ and that the following boundary conditions for the volume fraction m hold valid for $dm/dx = \text{constant} > 0$: $m(x_{\text{R}}) = 0$ and $m(x_{\text{T}}) = 1$.

Our further calculations were aimed at the determination of the ZNSPs (see formulae (7)–(9)) at the interfaces such as CF (figure 1). Surprisingly, many variants of such ZNSPs appear with variations of the parameters u_{R}, g_{R}, h_{T}, f_{M} and p_{M} (see section 2) which describe the volume fractions of the different domain types in the coexisting phases. It is important to note that any changes in the u_{R}, g_{R} and f_{M} values cannot strongly change the elastic matching conditions for the formation of the ZNSPs in the heterophase PZN–PT single crystals. Such an effect is explained by a negligible influence of the shear unit-cell distortions of the domains in the Rh and M$_{\text{C}}$ phases. Otherwise, this influence is expressed in terms of fairly small off-diagonal matrix elements (see equations (2) and (4)) depending on u_{R}, g_{R} or f_{M}. Among various orientations $\boldsymbol{n}_i(h_il_il_i)$ of the interfaces which are ZNSPs (see formulae (9)), we regard as most probable the interfaces parallel to the (100) or (010) plane of the perovskite unit cell. These interfaces are simultaneously parallel to the permissible domain (twin) walls [24] in the M$_{\text{C}}$ phase (see, for example, the CF line in figure 1) and, therefore, provide complete stress relief at the elastic matching of the two-phase regions of the ABCF and CDEF types.

The most interesting examples of the three-phase states in the PZN–PT single crystals are illustrated by concentration dependences $m_{\text{R}}(x_{\text{eff}})$, $m_{\text{M}}(x_{\text{eff}})$ and $m_{\text{T}}(x_{\text{eff}})$ (see formulae (1) and (10)) which were calculated (figure 2) for the ZNSP orientations close to the (100) or (010) planes of the perovskite unit cell. A transition from the heavily twinned Rh phase ($u_{\text{R}} = g_{\text{R}} = 1/2$; figure 2(a)) to the single-domain one ($u_{\text{R}} = g_{\text{R}} = 1$; figure 2(b)) results in increasing of the volume fractions m_{M} and m_{T} to some degree at $x_{\text{eff}} < 0.07$: this effect is explained by the active role of the mechanical twins of the M$_{\text{C}}$ and T phases in the stress relief near the morphotropic phase boundary. The above-mentioned changes in the 71° (109°) domain structure of the Rh phase practically do not affect the location of max $m_{\text{M}}(x_{\text{eff}})$ (compare curves 2 in figures 2(a) and (b)) and this fact attests to the passive role of the Rh phase in the stress relief at the phase coexistence.

The calculated curves shown in figure 2 are in good agreement with the experimental concentration dependences [17] found for the phases coexisting in the PZN–PT single crystals at $0.06 < x < 0.11$. In this connection, it should be noted that the unit-cell parameters and the volume fractions of the Rh, M$_{\text{C}}$ and T phases were measured by Bertram *et al* [17] for the same heterophase PZN–PT single crystals. This circumstance makes it possible to directly compare our calculation results (figure 2) and the experimental data [17]. The features of the three-phase states are successfully explained on the basis of the proposed model (figure 1) and the procedure for the determination of the ZNSPs at the elastic matching of the two-phase regions (equations (5)–(9)). Such or like combinations of the morphotropic phases were not considered in earlier papers on ferroelectrics and related materials and they enable us to characterize the PZN–PT solid solutions as a unique system in which the three-phase states '$\cdots$–(Rh + M$_{\text{C}}$)–(M$_{\text{C}}$ + T)–$\cdots$' would provide complete stress relief over a wide x range.
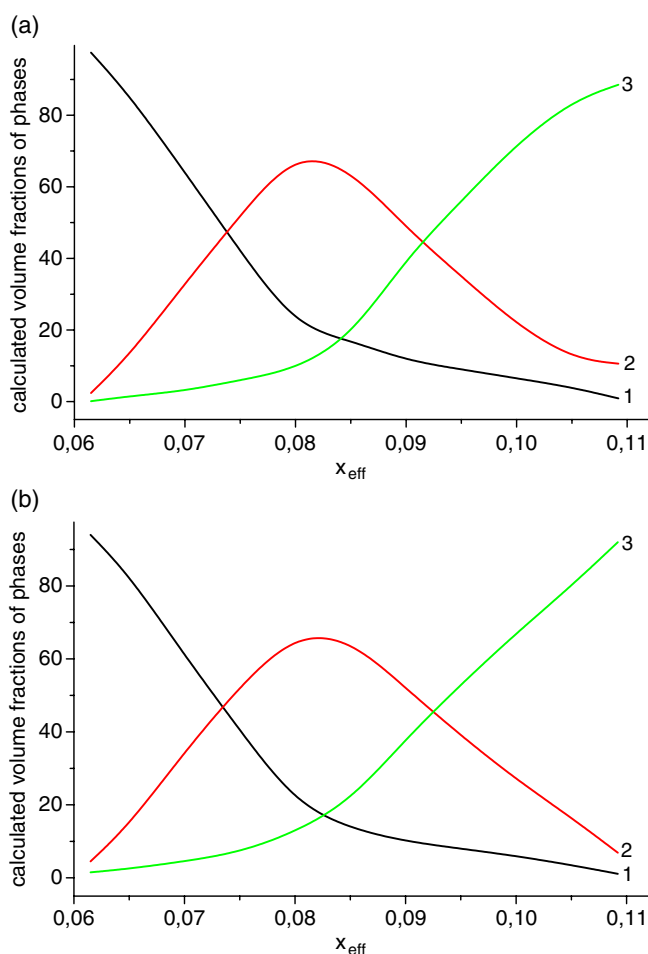
Figure 2. Calculated concentration dependences of the volume fractions $v_i(x_{eff})$ (in %) of the morphotropic phases in the PZN–PT single crystals containing the polydomain (a) or single-domain (b) Rh phase. Calculations were made for cases $u_R = g_R = 1/2$ (a) and $u_R = g_R = 1$ (b). In both cases, curves 1, 2 and 3 are related to $v_R(x_{eff})$, $v_M(x_{eff})$ and $v_T(x_{eff})$, respectively.

(This figure is in colour only in the electronic version)

4. Conclusions

Using the experimental data on the unit-cell parameters [17] and developing the concepts of ZNSPs in heterophase ferroelectrics [10, 11, 18–20], the three-phase states have been studied in the relaxor–ferroelectric PZN–PT single crystals near the morphotropic phase boundary. Progress has been achieved in modelling and crystallographically describing the heterophase systems with the ZNSPs on different levels, i.e., between the adjacent domains, the domain or twinned regions, the adjacent phases and the two-phase regions. Despite the lack of experimental data on features of heterophase/domain structures of the single crystals at various molar concentrations x, the volume fractions (1) of the morphotropic phases have been evaluated over a wide range of the x values and good correlation between the calculated and experimental results has been established. It is believed that the proposed model of the three-

phase states and the features of the elastic matching studied shed light on the morphotropic phase transitions in heavily twinned ferroelectric single crystals.

Acknowledgments

References

[1] Park S-E and Hackenberger W 2002 *Curr. Opin. Solid State Mater. Sci.* **6** 11
[2] Noheda B 2002 *Curr. Opin. Solid State Mater. Sci.* **6** 27
[3] Yin J, Jiang B and Cao W 2000 *IEEE Trans. Ultrason. Ferroelectr. Freq. Control* **47** 285
Jiang W, Zhang R, Jiang B and Cao W 2003 *Ultrasonics* **41** 55
[4] Topolov V Yu and Turik A V 2001 *Phys. Solid State* **43** 1117
Topolov V Yu and Turik A V 2002 *Phys. Solid State* **44** 1355
[5] Ren W, Liu S-F and Mukherjee B K 2003 *Appl. Phys. Lett.* **83** 5268
[6] Fuishiro K, Vlokh R, Uesu Y, Yamada Y, Kiat J-P, Dkhil B and Yamashita Y 1998 *Japan. J. Appl. Phys.* 1 **37** 5246
Ye Z-G, Dong M and Zhang L 1999 *Ferroelectrics* **229** 223
Ye Z-G and Dong M 2000 *J. Appl. Phys.* **87** 2312
[7] Topolov V Yu and Ye Z-G 2001 *Ferroelectrics* **253** 71
[8] Yin J and Cao W 2000 *J. Appl. Phys.* **87** 7438
[9] Iwata M, Araki T, Maeda M, Suzuki I, Ohwa H, Yasuda N, Orihara H and Ishibashi Y 2002 *Japan. J. Appl. Phys.* 1 **41** 7003
Iwata M, Katsuraya K, Suzuki I, Maeda M, Yasuda N and Ishibashi Y 2003 *Japan. J. Appl. Phys.* 1 **42** 6201
[10] Topolov V Yu 2002 *Phys. Rev.* B **65** 094207
[11] Topolov V Yu 2003 *Phys. Solid State* **45** 1295
[12] Noheda B, Cox D E, Shirane G, Park S-E, Cross L E and Zhong Z 2001 *Phys. Rev. Lett.* **86** 3891
[13] Vanderbilt D and Cohen M H 2001 *Phys. Rev.* B **63** 094108
[14] La-Orauttapong D, Noheda B, Ye Z-G, Gehring P M, Toulouse J, Cox D E and Shirane G 2002 *Phys. Rev.* B **65** 144101
[15] Kiat J-M, Uesu Y, Dkhil B, Matsuda D, Malibert C and Calvarin G 2002 *Phys. Rev.* B **65** 064106
[16] Uesu Y, Matsuda M, Yamada Y, Fujishiro K, Cox D E, Noheda B and Shirane G 2002 *J. Phys. Soc. Japan* **71** 960
[17] Bertram R, Reck G and Uecker R 2003 *J. Cryst. Growth* **253** 212
[18] Metrat G 1980 *Ferroelectics* **26** 801
[19] Topolov V Yu and Turik A V 1995 *Defect Diff. Forum* A **123/124** 31
[20] Topolov V Yu, Turik A V, Fesenko O E and Eremkin V V 1995 *Ferroelectr. Lett. Sect.* **20** 19
[21] Topolov V Yu 1998 *Crystallogr. Rep.* **43** 68
[22] Noheda B, Cox D E, Shirane G, Gonzalo J A, Cross L E and Park S-E 1999 *Appl. Phys. Lett.* **74** 2059
Noheda B, Cox D E, Shirane G, Guo R, Jones B and Cross L E 2001 *Phys. Rev.* B **63** 014103
[23] Topolov V Yu and Turik A V 2001 *J. Phys.: Condens. Matter* **13** L771
[24] Fousek J and Janovec V 1969 *J. Appl. Phys.* **40** 135
Fousek J 1971 *Czech. J. Phys.* B **21** 955
[25] Wada S, Park S-E, Cross L E and Shrout T R 1999 *Ferroelectrics* **221** 147
[26] Topolov V Yu, Balyunis L E, Turik A V, Bah I S and Fesenko O E 1992 *Bull. Russ. Acad. Sci. Phys.* **56** 1588